Marine Ice Sheet Instability and Ice Shelf Buttressing Influenced Deglaciation of the Minch Ice Stream, Northwest Scotland

Niall Gandy[1], Lauren J. Gregoire[1], Jeremy C. Ely[2], Christopher D. Clark[2], David M. Hodgson[1], Victoria Lee[3], Tom Bradwell[4], Ruza F. Ivanovic[1]

[1]School of Earth and Environment, The University of Leeds, Leeds, LS2 9JT, United Kingdom
[2]Department of Geography, The University of Sheffield, Sheffield, S10 2TN, United Kingdom
[3]School of Geographical Sciences, The University of Bristol, Bristol, BS8 1SS, United Kingdom
[4]Biological and Environmental Sciences, The University of Stirling, Stirling, FK9 4LA, United Kingdom

Correspondence to: Niall Gandy (eeng@leeds.ac.uk)

Abstract. Uncertainties in future sea level projections are dominated by our limited understanding of the dynamical processes that control instabilities of marine ice sheets. A valuable case to examine these processes is the last deglaciation of the British-Irish Ice Sheet. The Minch Ice Stream, which drained a large proportion of ice from the northwest sector of the British-Irish Ice Sheet during the last deglaciation, is well constrained, with abundant empirical data which could be used to inform, validate and analyse numerical ice sheet simulations. We use BISICLES, a higher-order ice sheet model, to examine the dynamical processes that controlled the retreat of the Minch Ice Stream. We simulate retreat from the shelf edge under constant "warm" surface mass balance and subshelf melt, to isolate the role of internal ice dynamics from external forcings. The model simulates a slowdown of retreat as the ice stream becomes laterally confined at a "pinning-point" between mainland Scotland and the Isle of Lewis. At this stage, the presence of ice shelves became a major control on deglaciation, providing buttressing to upstream ice. Subsequently, the presence of a reverse slope inside the Minch Strait produces an acceleration in retreat, leading to a 'collapsed' state, even when the climate returns to the initial 'cold' conditions. Our simulations demonstrate the importance of the Marine Ice Sheet Instability and ice shelf buttressing during the deglaciation of parts of the British-Irish Ice Sheet. Thus, geological data could be used to constrain these processes in ice sheet models used for projecting the future of our contemporary ice sheets.

1 Introduction

Attempts to model the future evolution of the West Antarctic Ice Sheet reveal large uncertainty in the extent of future mass loss (Feldmann and Levermann, 2015; Ritz et al., 2015). This is partly because many contemporary Antarctic Ice Streams are marine based (Jenkins et al., 2010; Joughin et al., 2014; Ross et al., 2012), and are therefore vulnerable to Marine Ice Sheet Instability (MISI). Schoof (2007) demonstrated that no stable grounding line position is possible in areas of reversed bed slope. This means that any change in ice thickness at the grounding line can cause an instability in grounding line migration. However, it has been shown that simulations of grounding line migration require not only consideration of bed topography, but also ice

shelf buttressing (Gudmundsson, 2013), as this mechanism can stabilise grounding lines on reverse sloping beds. The previous generation of ice sheet models do not accurately simulate the position of the grounding line, due to the use of the Shallow Ice Approximation (van der Veen, 2013). Higher-order models, such as used here, have various numerical approaches to solving ice flow, and have more success (Favier et al., 2014; Pattyn et al., 2012), but are still sensitive to model resolution (Cornford

5   et al., 2016) and the representation of basal sliding processes (Gladstone et al., 2017; Nias et al., 2016).

It is essential for improved future predictions of ice sheet change to better understand the dynamics of marine ice sheets over millennial timescales. A numerical simulation of the palaeo Marguerite Bay Ice Stream since the Last Glacial Maximum shows that the non-linear retreat was controlled by a combination of bed topography, ice stream width, and retreat history, and that these controls are crucial to understanding centennial ice sheet evolution (Jamieson et al., 2012). A valuable

10   case to examine these processes is the last deglaciation of the British-Irish Ice Sheet (BIIS), which had a number of marine-grounded sectors (Clark et al., 2012). While contemporary ice sheets offer a decadal scale observational record, the palaeo record of the BIIS provides detailed proxy-observations of ice sheet retreat over millennia. The behaviour of the BIIS has been studied for over a century, resulting in much information on flow patterns and margin positions against which ice-sheet models can be compared (Clark et al., 2018). Information on the timing and pace of retreat has been considerably enhanced through

15   the recent work of the BRITICE-CHRONO project, a multi-organization consortium, which has collected data to better constrain the timing of retreat of the BIIS, particularly in marine sectors. The data-rich environment that the empirical record now holds makes it an attractive test bed for numerical ice sheet modelling experiments (e.g. Boulton et al., 2003; Boulton and Hagdorn, 2006; Hubbard et al., 2009; Patton et al., 2016, 2017). The modelling investigations of Boulton et al. (2003) and Hubbard et al. (2009) specifically highlighted the importance of ice stream dynamics in the evolution of the ice sheet. However,

20   simulations of marine ice sheets, like the West Antarctic Ice Sheet or the BIIS, ideally require models that are able to simulate grounding line migration (Pattyn et al., 2012). The BISICLES ice sheet model was developed to efficiently and accurately model marine ice sheets (Cornford et al., 2013), allowing for new simulations of the BIIS which explore marine influence on the ice sheet.

We investigate the marine influence on one very well constrained ice stream of the BIIS, the Minch Ice Stream

25   (MnIS), using the BISICLES ice sheet model. Here, we perform and analyse numerical modelling simulations to test two hypotheses of MnIS retreat; (1) that the ice stream experienced MISI, and (2) that an ice shelf had an influential buttressing effect on the pace of retreat.

2 The Minch Ice Stream

The Minch Ice Stream (MnIS) flowed northward from the northwest Scottish Highlands through the Minch Strait

30   (Figure 1). It reached its maximum extent, the edge of the continental shelf, at ~30 ka BP (Bradwell et al., 2008), which we here refer to as the local Last Glacial Maximum (lLGM). The ice stream's flow was topographically constrained by the Outer Hebrides, and there is no geological evidence onshore or offshore that the ice stream migrated in position during the glacial

cycle (Bradwell et al., 2007). Empirical (Bradwell et al., 2008; Clark et al., 2012) and numerical-model based (Boulton and Hagdorn, 2006; Hubbard et al., 2009) studies show that this wide (~50 km) ice stream drained a large proportion of ice that accumulated over the Scottish Highlands. The MnIS trough can be divided into the outer trough, which is predominantly smooth, with low-strength sediments, and the inner trough with an undulating bed and reduced Early Quaternary sediment

5   cover (Figure 1). The inner trough contains a Neoproterozoic bedrock high, here referred to as a Mid-Trough Bedrock High (MTBH) (Figure 1). Either side of the MTBH, the Minch branches into east and west troughs (Figure 1).

There has been extensive onshore (Ballantyne and Stone, 2009; Bradwell, 2013) and offshore (Bradwell and Stoker, 2015; Bradwell et al., 2008; Stoker and Bradwell, 2005) studies of the MnIS catchment. Improved bathymetry data allow the identification of a reverse slope southward of the MTBH. This topography could facilitate MISI, potentially causing rapid

10 retreat south of the MTBH, and would explain the relative sparsity of the landform record between the MTBH and the terrestrial transition (Bradwell et al., 2008; Clark et al., 2018). Numerical modelling also allows for ice sheet processes to be tested that may be less evident in the empirical record, such as the influence of ice shelves. The detailed reconstructions of the MnIS provide an excellent opportunity to test whether ice-sheet models reproduce behaviour expected from the empirical data.

3 Methods

15 ### 3.1 Model description and set-up

We use the BISICLES ice sheet model (Cornford et al., 2013) to simulate the MnIS. BISICLES is a higher-order ice sheet model with Schoof-Hindmarsh L1L2 physics (Schoof and Hindmarsh, 2010), which was developed to efficiently and accurately model the dynamics of marine-grounded ice sheets. It uses adaptive mesh refinement to automatically increase resolution at high velocities and the grounding line, allowing ice stream dynamics and grounding line migration to be well

20 represented, while having a lower resolution in the rest of the ice sheet ensures efficient model speed. Cornford et al. (2013) provides a full description of BISICLES. Although our focus for analysis is the MnIS, we set up the model domain to cover the majority of the British-Irish Ice Sheet (BIIS) at 4 km x 4 km resolution, excluding the central North Sea (Figure 2). Simulating a large portion of the BIIS prevents artefacts caused by domain boundary effects, and allows for migration of ice catchments during deglaciation. For the set-up of the study, we set a 4 km x 4 km grid refined 3 times around the grounding

25 line in the Minch Sector to produce a maximum horizontal resolution of 500 m x 500 m. The simulations have 10 vertical levels. The friction law uses a linear ($m = 1$) Weertman exponent. We use a calving model that simulates frontal ablation by advecting the calving front with a relative velocity equal to the modelled ice velocity at the front minus an ablation rate acting in a direction normal to the front. We prescribe a frontal ablation rate of 250 m/y for all lLGM simulations, and 350 m/y for all simulations which prompt deglaciation. These frontal ablation values are prescribed as it allows for a stable extent at the

30 continental shelf edge, and causes only limited deglaciation if Surface Mass Balance (SMB) changes are not included (Figure S2).

3.2 Initial conditions and spin-up

For the purpose of this study, we set the starting point of our simulations as when the MnIS reached its maximum extent. To avoid the computational costs and uncertainties associated with simulating the full build-up of the ice sheet, we initialise ice thickness in the domain from a perfectly plastic ice sheet model (Gowan et al., 2016) fixed to the lGGM extent at

5   the continental shelf break. For the purposes of this study, the 27ka BP margin of Clark et al. (2012) was used for the remainder of the BIIS, fortunately the 27 ka BP margins of the perfectly plastic ice sheet model output match well with the reconstructed maximum extent of the MnIS (Bradwell et al., 2008).

To calculate SMB we use monthly mean surface air temperatures and monthly mean total precipitation from climate model simulations to drive a Positive Degree Day (PDD) mass balance model, as described by Seguinot (2013) and Gregoire

10   et al. (2016, 2015). The PDD model is driven by mean temperature and precipitation data calculated from the final 50-years of the 26 ka BP bias-corrected equilibrium climate simulation described by Morris et al. (2018), run with the HadCM3 coupled atmosphere-ocean-vegetation general circulation model (Gordon et al., 2000; Pope et al., 2000; Valdes et al., 2017). This simulation is part of a series of "snapshot" equilibrium simulations covering the last deglaciation that are a refinement of those previously reported by Singarayer et al. (2011) with updated boundary conditions (Ivanovic et al., 2016). It belongs to the

15   same set of simulations used by Swindles et al. (2017) to recently derive Holocene climate. We downscale surface air temperatures onto the pre-spin up initial ice sheet surface using a lapse rate of 5.1 K/km, which has been identified as a suitable lapse rate for modelling the Eurasian Ice Sheet (Siegert and Dowdeswell, 2004).

To remove the effect of a SMB feedback, where surface elevation change causes a positive feedback to SMB due to atmospheric lapse rate, the SMB is decoupled from elevation feedback. In practice, this means that once surface air

20   temperatures are downscaled onto the initial ice sheet surface elevation to create the SMB map for the domain, SMB does not evolve as the ice sheet surface elevation evolves; there is no lapse rate feedback. This removes the possibility for a SMB instability of retreat, allowing for the internal instabilities of the ice sheet to be isolated.

We prescribe a sub-shelf melt rate using a linear relationship with Sea Surface Temperature (SST); sub-shelf melt (m/y) is 10× the annual average SST (K) above the freezing point of seawater, taken to be -1.8 °C. This relationship between

25   SST and sub-shelf melt rate is based on measurements from Pine Island Glacier, Antarctica (Iyengar et al., 2001). SST values are taken from the same climate simulation that is used to calculate SMB. However, initial SST temperatures are corrected by -2 ºC as exploratory sensitivity tests show that the uncorrected SST does not allow for ice shelves to form at the lGGM. We correct the SST to permit for ice shelf formation, allowing the influence of the presence or removal of an ice shelf to be tested.

We assume that contemporary land properties are like the bed properties beneath the MnIS, and we use a bed friction

30   map reconstruction which parcelled together areas of similar bed friction using a combination of sediment thickness, palaeo ice stream location, and subglacial bedforms (Supplementary Information 3). The values for bed friction coefficients used as input into BISICLES (Figure 2c) were based on studies of present day ice streams using the same friction law Weertman exponent ($m = 1$), which calculated coefficients by inverting observed surface velocity (Favier et al., 2014; Gong et al., 2017).

This approach simulates an ice stream of a similar magnitude as reconstructed using empirical data (Bradwell et al., 2007). Sensitivity tests reveal that the ice sheet volume is sensitive to changes in bed friction coefficient map (Figure S1), but the extent of ice after a 6,000 year spin-up remains comparable even with different magnitudes of basal friction.

To recreate isostatically adjusted bed topography, we adjust modern topography using a Glacio-Isostatic Adjustment (GIA) model (Figure 2d). GEBCO (Becker et al., 2009) provides modern offshore bathymetry, and SRTM (Farr et al., 2007) provides onshore topography. Isostatic adjustment was simulated using the EUST3 GIA model (Bradley et al., 2011). EUST3 accounts for near-field and far-field isostatic adjustment due to ice loading. The Relative Sea Level (RSL) change from EUST3 at 30ka BP is used to deform contemporary topography, maintaining a high resolution ice sheet bed whilst also accounting for RSL change.

3.3 Experimental design

We designed our experiments to use an idealised representation of the external forcings of ice sheet retreat (surface mass balance and sub-shelf melt) in order to isolate the internal ice sheet mechanisms and instabilities of retreat. All experiments begin at a stable lLGM volume, with continental shelf edge glaciation and a small ice shelf (<4 km from shelf front to the grounding line) (Figure 3). Experiment set-up is summarised in the supplement (Table S1).

3.3.1 Deglaciation

In the simulation *RETREAT,* we use an idealised climate perturbation approach to trigger deglaciation, which consists of applying an instantaneous uniform warming of the surface air temperature by 1.5 K and SST by 2 K each month, without changing precipitation. The resulting surface mass balance and sub-shelf melt are then kept constant throughout the run. As for the *SPINUP* simulation, SMB is decoupled from an ice elevation-SMB feedback. Therefore, any change in the rate of ice sheet retreat is caused by internal ice sheet dynamics.

To test the relative role of ocean and atmospheric warming in driving the retreat, we ran *RETREAT_ATMOS* and *RETREAT_OCN* where only SMB or sub-shelf melt rate are perturbed respectively. Both of these simulations only lead to partial deglaciation (Figure S2), while the combination of both forcings (*RETREAT*) cause deglaciation to the northwest Scottish Highlands. We keep bed topography and sea level constant for the duration of the deglaciation simulations as the purpose of the study is to test for a retreat instability of the MnIS with a given topography. This prevents RSL change exaggerating or dampening any simulated instabilities as it would have done during the last deglaciation.

3.3.2 Reversibility of ice stream retreat

We test whether retreat is irreversible once it is initiated, or whether ice volume and area recovers to lLGM levels given a return to lLGM climate. In experiment *READVANCE,* we test for the reversibility of ice stream retreat by reverting the climate perturbations during the deglaciation. A set of simulations were started from points at 800 years intervals through the *RETREAT* simulation with the boundary conditions returned to lLGM and run for 10,000 model years to allow the ice sheet to

reach a new stable state (constant volume and extent). Here, ice sheet collapse is defined as an ice sheet not returning to its lLGM extent given lLGM boundary conditions following retreat.

3.3.3 Ice shelf influence

We tested whether an ice shelf is important in influencing the dynamics of the MnIS retreat, by providing a buttressing force to reduce ice stream flux over the grounding line. To test this hypothesis, we ran a simulation (*RETREAT_NOSHELF*) where the sub-shelf melt rate was increased to 100 m/y (52.9 m/y higher than during the *RETREAT* simulation) in order to force the removal of the ice shelf during deglaciation. Note that, in this experiment, we kept the frontal ablation rates identical to *RETREAT* in order to isolate the effects of ice shelf buttressing, removing the influence of any increased ocean ice mass loss.

4 Results and Discussion

4.1 Pattern of retreat

Imposing a constant SMB and sub-shelf melt perturbation (simulation *RETREAT*) causes a retreat of the MnIS from the continental shelf edge to the highlands within 8,000 model years (Figure 4; Video S4). Although the SMB and sub-shelf melt are constant through the simulation, with SMB decoupled from the change in surface elevation, the rate of volume and area change is not constant through the simulation (Figure 4a). The evolution of the ice stream during the RETREAT simulation can be divided into three stages; an initial retreat phase, a stagnation phase, and a late retreat phase. Volume loss is most rapid at the initial retreat phase (Figure 4b-d), halving the domain's ice volume in the first 2,000 model years of the simulation. In the stagnation phase, between 2,000 and 6,300 model years of the simulation (Figure 4d-e), volume loss slows. Finally, during the late retreat phase volume loss slightly increases from 6,300 model years onwards (Figure 4e-f). The slower rate of volume loss in the stagnation phase occurs as the margin retreats beyond marine influence onto the Outer Hebrides for the majority of the domain, and the re-acceleration of the late retreat phase only begins once the grounding line has retreated further south towards the inner trough of the Minch Strait (Figure 4e).

The ice area loss produces a broadly similar trend to volume loss, although in the stagnation phase (3,500 to 6,300 model years) there is negligible area loss despite continuing volume loss (Figure 4a). This is associated with a near-stagnation of the grounding line when the margin of the ice sheet has mostly retreated onshore and the marine-terminating ice stream becomes confined between the Scottish mainland and the Outer Hebrides (Figure 4d-e). During the stagnation phase ice loss occurs through thinning with limited change in margin position. As the thinning continues the ice area begins to retreat more rapidly just after 6,300 model years, which coincides with the start of a rapid margin retreat in the Minch (figure 4e).

4.2 Role of ice shelf buttressing

Ice shelves provide a buttressing membrane stress to the ice streams flowing upstream of them (Hindmarsh, 2006), and the result of the sudden collapse of ice shelves has been observed in the contemporary Antarctic Peninsula (Scambos et al., 2004). The buttressing effect of ice shelves can also allow a stable grounding line position given a reverse sloping bed

5   (Gudmundsson, 2013), meaning it is important to consider the impact of ice shelves when examining MISI. The ice shelf that forms during the simulations of the MnIS is initially unconstrained by topography or surrounding ice until the grounding line retreats during the stagnation phase of retreat at 6,300 years (Figure 4e). It is therefore expected that removing the ice shelf from the simulations whilst triggering deglaciation will initially have negligible impact on the retreat of the ice stream, before having greater impact once the ice shelf is constrained by surrounding grounded ice.

10 For the first 5,000 model years the simulated ice volumes diverge by less than 1% in the simulations with (*RETREAT*) and without (*RETREAT_NOSHELF*) an ice shelf (Figure 5). After 5,000 model years there is a notable divergence in the evolution of ice volume of the two simulations, where the simulation without an ice shelf has higher rates of mass loss compared to the simulation with ice shelves (Figure 5a). At the time of maximum volume difference between the simulations (7,000 model years), the simulation *RETREAT_NOSHELF* has a volume ~2,000 km^3 (10%) smaller than the simulation

15 *RETREAT*. However, the acceleration of mass loss during the late retreat phase occurs in both simulations, suggesting the presence or removal of an ice shelf cannot prevent continued ice volume loss. Although the presence of an ice shelf affects the ice volume, it has almost no impact on the location of the grounding line and its chronology of retreat (e.g. Figure 5b-c), with the difference in the grounding line location mostly within the finest resolution of the model (500 m). The removal of the ice shelf also means that the grounding line has no mechanism for stability on the reverse sloping bed retreat southward of the

20 MTBH (Gudmundsson, 2013). These results suggest that although the presence or absence of an ice shelf has a limited influence on the spatial pattern and timing of MnIS retreat, the volume change caused by removing an ice shelf is significant. A significant difference in ice volume is not reflected in grounding line position, showing that ice flux across the grounding line is important, not just the position of the grounding line. The significance of the ice shelf influence demonstrates that in order to be confident of the future evolution of our contemporary ice sheets, we need to be confident of the future evolution of

25 ice shelves over centennial timescales.

The unconstrained nature of the Minch Ice Shelf at the start of the deglaciation makes the mechanics of ice shelf buttressing different from many areas of the contemporary West Antarctic Ice Sheet, where large ice shelves are buttressed laterally by surrounding ice or bedrock (Pritchard et al., 2012). In a number of prominent places in Antarctica, ice shelves are also pinned from underneath by bedrock rises (Matsuoka et al., 2015). This may suggest that the dynamics of the Minch Ice

30 Shelf during the first stage of retreat are more analogous to East Antarctic Ice Shelves. The Minch Ice Shelf is not constrained laterally until the later stages of the deglaciation where the shelf is supported by surrounding ice (Figure 5), where the topographic setting is similar to examples of fjord-like confined glaciers in Greenland (Joughin et al., 2008). Whilst the MnIS and many Greenland ice streams can retreat beyond direct marine influence (Funder et al., 2011), this is not possible for

Antarctic ice streams grounded in deeper troughs. Empirical evidence of the last Eurasian ice sheet has the western ice margin constrained by the continental shelf edge across the majority of the Atlantic margin (Hughes et al., 2016). This suggests that ice shelves at maximum ice extent across the Atlantic margin would be similar to the Minch Ice Shelf in the early stages of deglaciation, limited in size by the continental shelf break, and unconstrained. It is likely, therefore, that ice shelves along this

5   Atlantic margin were not influential in the retreat of the ice sheet until the grounding line retreated to areas laterally constrained by topography or surrounding ice.

4.3 Testing ice stream instability with readvance experiments

Given the bathymetric profile of the ice stream path (Figure 6), it would be expected that the MnIS would experience MISI ~180 km along the AB transect (Figure 6b). This is because of the reverse slope (downhill retreat) that the ice stream

10   path would encounter in the later stages of the deglaciation after retreating beyond the MTBH. The experiment *READVANCE* returns the ice stream to the lLGM climate at 800 year intervals during the *RETREAT* experiment, in an attempt to recover the ice stream to lLGM extent.

For the first 5,600 model years of the recovery experiment (*READVANCE*) ice volume returns to lLGM extent given a return to lLGM forcings. All simulations started from *RETREAT* at model year 800 to 5,600 readvance to the lLGM extent.

15   However, in simulations with a point of recovery (initial conditions) beyond 5,600 model years, the ice stream does not recover to lLGM extent given lLGM boundary conditions (Figure 7a,b); instead it evolves towards a reduced stable state with a volume ~25% smaller, and an area ~50% smaller than the stable lLGM state (Figure 7d).

We identify two stable ice conditions in these *READVANCE* simulations given our initial lLGM forcings; a full shelf-edge glaciation, and a small Hebrides Ice Cap with glaciation in the Minch limited to the east trough (Figure 7). The resulting

20   stable extent of the ice stream is dependent on the evolution history of the ice stream; there is hysteresis in the MnIS evolution. Hysteresis of ice sheet evolution is evidence for an instability during the advance of retreat of an ice sheet (Schoof, 2007). Ice sheets can experience a variety of instabilities (Calov et al., 2002; Gregoire et al., 2016, 2012; Schoof, 2007) which could influence the ice sheet evolution.

The zone of collapse is defined here as the point of divergence of recovery states; the position of the grounding line

25   at which returning to lLGM forcing no longer allows recovery to initial lLGM extent, and only allows recovery to the new stable condition of limited Minch glaciation (Figure 7d). The zone of collapse occurs 5,600-6,400 model years into the retreat, ~180 km along the mapped AB transect (Figure 6). The AB transect shows that for the majority of the deglaciation the ice stream is retreating "uphill" from the continental shelf edge. A reverse slope is present from ~180 km along the AB transect (Figure 6). The point of collapse is simulated to occur after the margin has retreated back from the MTBH. The results of the

30   *READVANCE* simulations suggest that the MnIS transitions through a zone of instability when its grounding line retreated past the MTBH on a reverse slope, thus indicating that the observed hysteresis is caused by MISI.

As well as the influence of MISI, the morphology of the ice stream margin may also cause an instability during the retreat of the ice stream. For the majority of the retreat, the ice stream is buttressed to the east and west by surrounding ice

(Figure 4). However, in the smaller stable state (Figure 7d), the ice stream is not buttressed on the western margin, due to the bay forming in the west trough of the Minch. This removal of the lateral buttressing of the ice stream to the west may also contribute to the inability of the ice stream to recover the lLGM extent in this experiment.

The difference between the grounding line position at the zone of transition and at the collapse state, the magnitude of collapse, varied across the ice stream (Figure 8a). In the east of the trough the magnitude of collapse was limited, and a bathymetric transect shows only a limited reverse slope to facilitate MISI (Figure 8b). However, in the west of the trough the magnitude of collapse was more significant, and the bathymetric transects shows a more sustained reverse slope to facilitate MISI (Figure 8c).

With ice unable to advance beyond the MTBH in the recovery simulations, a mechanism is required to allow ice to first advance towards the shelf edge prior to the lLGM, but then be unable to advance after retreat from lLGM extent. Although this study started with an ice extent already at the lLGM extent, other studies such as Patton et al. (2016) successfully simulated the build-up of the entire Eurasian ice sheet, with ice overcoming the MTBH and reaching the shelf edge given an lLGM climate. The variability and uncertainty in the climate forcing could allow readvance back to the continental shelf edge. In particular, in our model, if the lLGM climate is uniformly cooled by 0.5 K across the entire domain ice readvances from a "collapsed" position to an lLGM position. It is reasonable that this small correction falls within the error of the climate simulations or variability in the climate during the build-up phase. Nonetheless, even with the cooled climate, recovery back to lLGM extent is considerably slower beyond 5,600 model years. Despite cooling the climate to force a recovery to lLGM extent, a behavioural change in the ice stream readvance beyond 5,600 model years remains.

Topographic changes over the course of the glacial cycle may also explain why the simulations did not readvance over the MTBH given lLGM conditions. These topographic changes would be present in two ways; changes in isostasy during the glacial cycle, and bed erosion and deposition. The simulations run on an ice sheet bed adjusted for isostacy at 30ka BP, which exaggerates the reverse slope causing MISI. The original advance of the ice stream would likely be on a bed where the slope was reduced. Bed erosion could also increase the prominence of the hard bedrock topographic high after initial glaciation. According to the modelling of Patton et al. (2016), MnIS is an area with high potential cumulative erosion 37-19ka BP. Both these mechanisms could exaggerate the reverse slope subsequent to glaciation, potentially allowing initial glacial advance, but not readvance from a retreated state. Therefore, this demonstrates the importance of understanding future topography evolution in understanding the long-term evolution of out contemporary ice sheets.

4.4 Comparison to observed retreat

The resulting pattern of retreat from the *RETREAT* simulation has a number of similarities with previous retreat reconstructions (Bradwell et al., 2008; Clark et al., 2012; Hughes et al., 2016) despite the idealised nature of the climate forcing. For example, the margin appears to "hinge" on the northern point of the Isle of Lewis (Bradwell et al., 2007). The margin also recesses into the Minch, with a small ice cap on the Outer Hebrides persisting during deglaciation. Due to the idealised climate forcing, only the pattern, and not the timing, of the retreat can be compared to empirical reconstructions.

There are close similarities between the simulated retreat and reconstructed retreat in the later stages of the deglaciation. In the later stages of retreat, both in the reconstructed and simulated retreat, the east trough contains a small ice stream whilst the west trough has fully deglaciated and formed a calving bay. We take the key similarities of retreat pattern and margin morphology between the simulated deglaciation and empirical deglaciation reconstructions as an indication that the main mechanisms that controlled the deglaciation of MnIS are replicated in our simulations.

All simulations in this study use constant climate forcing which do not account for the evolution of climate during the deglaciation of the BIIS. The fluctuations in volume and area change in the simulations are the signal of internal dynamical ice sheet processes, which do not include the feedback between SMB and elevation or any transient evolution of external forcing in climate and sea level. Here, we define the reconstructed retreat from the geomorphological and sedimentological evidence as the "observed retreat".

The observed retreat of the MnIS is the result of both the ice sheet internal and external forcing signal. Therefore, the signals simulated in these experiments could be exaggerated or dampened by external forcing; the climate signal. This style of retreat is evident from the moraine record (Figure 1), which shows a series of back stepping moraines across the continental shelf (Bradwell et al., 2008; Clark et al., 2018) It is inferred that these moraines form during a period of relative stability of the margin. These Grounding Zone Wedges occur in several places across the shelf edge, but there is only one period during the *RETREAT* simulation when the margin is stable, when the margin passes the northernmost tip of Lewis and enters the Minch (Figure 4 a and d). The surface expressions of the Grounding Zone Wedges are present in the bed topography used in the simulations. However, the ice margin retreats over other areas with a greater surface expression than Grounding Zone Wedges with no stabilisation of the margin. Based on our results, we suggest that GZW6 could have been caused by topographic influence, while the other GZWs are expressions of the climate signal.

The area and volume loss acceleration during the late retreat phase, which we interpret as the beginning of MISI, would also be influenced by the climate fluctuations during the observed retreat. The magnitude of this area and volume loss would be exaggerated or dampened depending on the increasing or decreasing SMB of the ice sheet at any given period. Overall, the simulated volume and area change in these simulations is relatively smooth, whilst during the observed retreat climate fluctuations will have caused annual or even decadal dynamic margin fluctuations, more akin to the Hubbard et al. (2009) simulation of the ice sheet evolution which was driven by a transient climate.

Geomorphological studies of palaeo ice sheets are able to reconstruct the area of ice sheets. Reconstructing ice thickness, and therefore volume, requires the introduction of further uncertainties, like bed friction and SMB, and therefore it is sometimes assumed that area change can directly inform volume change of the ice sheet (Hughes et al., 2016). However, model simulations of palaeo ice sheets can consider both area and volume changes. In these simulations although volume and area evolution showed a similar trend, the area evolution during *RETREAT* had more obvious pauses and accelerations in area loss than the pattern of volume loss. In this example, understanding the area change through geomorphic empirical evidence may overstate the magnitude of changes expected in volume loss.

An idealised climate warming perturbation was used to trigger deglaciation in the simulations (e.g. *RETREAT*) in order to isolate the internal mechanisms of retreat. However, the observed retreat began at ~30ka BP, when the NGRIP δ18O record suggests a cooling climate globally rather than a warming climate (Andersen et al., 2004). The warming mechanism we used to trigger deglaciation in our simulations is not apparent in the climate record. The results of the *RETREAT* simulations

5 also indicate that internal dynamical mechanisms alone would not have been sufficient to continue retreat until the triggering of MISI when the ice stream retreats past the MTBH. It seems that the MnIS was retreating in a cooling climate, these simulations idealised climate forcing to isolate internal ice sheet instabilities, and therefore do not reveal a mechanism that explains MnIS retreat in a cooling climate. There are two likely possibilities that could explain the MnIS retreating in a cooling climate (explained below); i) internal mechanisms caused by the expansion of the rest of the BIIS, or ii) a local SMB change

10 of this sector of the ice sheet at 30ka BP.

A local SMB change could be caused by atmospheric warming or a reduction in precipitation. Local warming of the northern British Isles, whilst the rest of the BIIS and other northern hemisphere ice sheets expanded, could be a mechanism to explain early MnIS retreat. The NGRIP ice core is more than the synoptic scale away from the Minch, and there could reasonably be local warming during global cooling. Given the uncertainty in palaeo climate modelling, particularly at high

15 latitude due to sensitivity to ice-sheet forcing (Singarayer and Valdes, 2010), it is a reasonable possibility that a local warming would not be included in the HadCM3 last glacial simulations used to force the ice sheet model. However, it seems unlikely that climate could be warming in the Minch whilst allowing rapid expansion for the remainder of the BIIS. Additionally, a local reduction in precipitation could be caused by a change in the position of the polar front, which would have been affected by the advance and retreat of the northern hemisphere ice sheets during the last glacial cycle (Oster et al., 2015). A migration

20 in the polar front would likely affect the entire western margin of the BIIS, potentially causing the start of deglaciation to be asynchronous with the rest of the northern hemisphere. However, as the forcing in these experiments remains idealised, this is only a speculative driver of early BIIS retreat.

Alternatively, internal mechanisms of the BIIS that were not simulated as part of this study could explain a retreating MnIS in a cooling climate. The simulations presented here did not feature a lapse rate effect on SMB as the ice sheet surface

25 lowered into a warmer climate. This process could help facilitate rapid retreat in a cooling climate, but could not be a trigger for retreat. During the retreat of the MnIS, ice was extending over Northern Ireland out to the shelf edge (Clark et al., 2012; Dunlop et al., 2010). It is theorised that a significant proportion of the ice feeding this advance came from the Hebrides Ice Stream, evidenced by large moraines northward of Donegal Bay. The source of the Barra Fan Ice Stream will have significantly overlapped with the MnIS, and the advance of the Barra Fan Ice Stream could have initiated ice piracy from the MnIS, causing

30 retreat in a cooling climate. This mechanism is speculative, and would require experiments with transient forcings to test. These internal instabilities would not have been represented in these simulations because a warming climate was used to trigger deglaciation, forcing the Barra Fan Ice Stream to retreat rather than advance. Bed friction and topography also do not evolve during the simulation, meaning ice streams in the simulations cannot activate or shutdown due to sediment exhaustion, or bed

hydrology changes. These simulations therefore provide evidence for internal processes during the retreat of the MnIS, but the initial trigger of deglaciation of the MnIS in a cooling climate remains elusive.

5 Conclusions

We simulated the retreat of the MnIS from a position of maximum extent, using an idealised climate perturbation in order to identify the role of the internal dynamical mechanisms of ice sheet retreat. This simulation showed a retreat in three phases, an initial retreat (0-3,500 model years), stagnation (3,500-6,300 model years), and a late retreat (after 6,300 model years). The stagnation phase occurred as the ice stream retreated past the northernmost tip of the Isle of Lewis. This slowing of volume and area loss coincides with a significant proportion of the margin retreating onto the Outer Hebrides, beyond marine influence. During this phase, a laterally constrained ice shelf provided buttressing to the ice stream. In the late retreat phase, the area and volume loss rate re-accelerated as the grounding line retreated on a reverse slope. We reversed the idealised climate perturbation regularly during this simulated deglaciation to test for instabilities of retreat. After the re-acceleration of volume and area loss at 6,300 model years, the ice sheet did not recover to lLGM volume and area given lLGM conditions. This result is evidence for a rapid retreat of the MnIS caused by marine ice sheet instability.

We compared the simulated retreat to a simulation with the ice shelves removed, which was otherwise identical. The simulations show that ice shelves were not influential to the magnitude and pattern of retreat for the first 5,000 model years of the simulated deglaciation, when the ice shelf was unconstrained. Once the margin had retreated into a geometry that constrained the ice shelf, the removal of the ice shelf caused higher ice stream velocities and a more rapid ice volume loss. We therefore find evidence for an influential ice shelf buttressing effect during the MnIS deglaciation. Our simulations demonstrate the importance of the MISI and ice shelf buttressing during the retreat of the Minch ice stream. These processes currently represent the largest source of uncertainty in projecting the future evolution the Antarctic ice sheet. We suggest that the detailed chronology of retreat of the British and Irish ice sheet currently produced by the BRITICE-CHRONO project has the potential to constrain important processes controlling MISI in models used for future sea level projections.

Competing interests. The authors declare that they have no conflict of interest.

Acknowledgements. NG was funded by a studentship from the Natural Environment Research Council (NERC) SPHERES Doctoral Training Partnership (NE/L002574/1) with CASE support from the British Geological Survey. This work was undertaken on ARC3, part of the High Performance Computing facilities at the University of Leeds, UK. JCE, CDC and TB were funded by the NERC consortium grant; BRITICE-CHRONO NE/J009768/1. RFI was supported by a NERC Independent Research Fellowship (NE/K008536/1). This work has benefited from extensive discussions with the BRITICE-CHRONO consortium team.

References

Andersen, K.K., Azuma, N., et al., 2004. High-resolution record of Northern Hemisphere climate extending into the last interglacial period. Nature 431, 147–151. https://doi.org/10.1038/nature02805

Ballantyne, C.K., Stone, J.O., 2009. Rock-slope failure at Baosbheinn, Wester Ross, NW Scotland: age and interpretation. Scottish J. Geol. 45, 177–181. https://doi.org/10.1144/0036-9276/01-388

Becker, J.J., Sandwell, D.T., et al., 2009. Global Bathymetry and Elevation Data at 30 Arc Seconds Resolution: SRTM30_PLUS. Mar. Geod. 32, 355–371. https://doi.org/10.1080/01490410903297766

Boulton, G., Hagdorn, M., 2006. Glaciology of the British Isles Ice Sheet during the last glacial cycle: form, flow, streams and lobes. Quat. Sci. Rev. 25, 3359–3390. https://doi.org/10.1016/j.quascirev.2006.10.013

Boulton, G.S., Hagdorn, M., Hulton, N.R.J., 2003. Streaming flow in an ice sheet through a glacial cycle. Ann. Glaciol. 36, 117–128. https://doi.org/10.3189/172756403781816293

Bradley, S.L., Milne, G.A., et al., 2011. An improved glacial isostatic adjustment model for the British Isles. J. Quat. Sci. 26, 541–552. https://doi.org/10.1002/jqs.1481

Bradwell, T., 2013. Identifying palaeo-ice-stream tributaries on hard beds: Mapping glacial bedforms and erosion zones in NW Scotland. Geomorphology 201, 397–414. https://doi.org/10.1016/j.geomorph.2013.07.014

Bradwell, T., Stoker, M., Larter, R., 2007. Geomorphological signature and flow dynamics of The Minch palaeo-ice stream, northwest Scotland. J. Quat. Sci. 22, 609–617. https://doi.org/10.1002/jqs.1080

Bradwell, T., Stoker, M.S., 2015. Submarine sediment and landform record of a palaeo-ice stream within the British-Irish ice sheet. Boreas 44. https://doi.org/10.1111/bor.12111

Bradwell, T., Stoker, M.S., et al., 2008. The northern sector of the last British Ice Sheet: Maximum extent and demise. https://doi.org/10.1016/j.earscirev.2008.01.008

Calov, R., Ganopolski, A., et al., 2002. Large-scale instabilities of the Laurentide ice sheet simulated in a fully coupled climate-system model. Geophys. Res. Lett. 29, 69-1-69–4. https://doi.org/10.1029/2002GL016078

Clark, C.D., Ely, J.C., et al., 2018. BRITICE Glacial Map, version 2: a map and GIS database of glacial landforms of the last British-Irish Ice Sheet. Boreas 47, 11-e8. https://doi.org/10.1111/bor.12273

Clark, C.D., Hughes, A.L.C., et al., 2012. Pattern and timing of retreat of the last British-Irish Ice Sheet. Quat. Sci. Rev. 44, 112–146. https://doi.org/10.1016/j.quascirev.2010.07.019

Cornford, S.L., Martin, D.F., et al., 2016. Adaptive mesh refinement versus subgrid friction interpolation in simulations of Antarctic ice dynamics. Ann. Glaciol. 57, 1–9. https://doi.org/10.1017/aog.2016.13

Cornford, S.L., Martin, D.F., et al., 2013. Adaptive mesh, finite volume modeling of marine ice sheets. J. Comput. Phys. 232, 529–549. https://doi.org/10.1016/j.jcp.2012.08.037

Dunlop, P., Shannon, R., et al., 2010. Marine geophysical evidence for ice sheet extension and recession on the Malin Shelf: New evidence for the western limits of the British Irish Ice Sheet. Mar. Geol. 276, 86–99.

https://doi.org/10.1016/j.margeo.2010.07.010

Farr, T.G., Rosen, P.A., et al., 2007. The Shuttle Radar Topography Mission. Rev. Geophys. 45, RG2004. https://doi.org/10.1029/2005RG000183

Favier, L., Durand, G., et al., 2014. Retreat of Pine Island Glacier controlled by marine ice-sheet instability. Nat. Clim. Chang. 4, 117–121. https://doi.org/10.1038/nclimate2094

Feldmann, J., Levermann, A., 2015. Collapse of the West Antarctic Ice Sheet after local destabilization of the Amundsen Basin. Proc. Natl. Acad. Sci. U. S. A. 112, 14191–6. https://doi.org/10.1073/pnas.1512482112

Funder, S., Kjeldsen, K.K., et al., 2011. The Greenland Ice Sheet During the Past 300,000 Years: A Review. Dev. Quat. Sci. 15, 699–713. https://doi.org/10.1016/B978-0-444-53447-7.00050-7

Gladstone, R.M., Warner, R.C., et al., 2017. Marine ice sheet model performance depends on basal sliding physics and sub-shelf melting. Cryosph. 11, 319–329. https://doi.org/10.5194/tc-11-319-2017

Gong, Y., Zwinger, T., et al., 2017. Importance of basal boundary conditions in transient simulations: Case study of a surging marine-terminating glacier on Austfonna, Svalbard. J. Glaciol. 63, 106–117. https://doi.org/10.1017/jog.2016.121

Gordon, C., Cooper, C., et al., 2000. The simulation of SST, sea ice extents and ocean heat transports in a version of the Hadley Centre coupled model without flux adjustments. Clim. Dyn. 16, 147–168. https://doi.org/10.1007/s003820050010

Gowan, E.J., Tregoning, P., et al., 2016. ICESHEET 1.0: a program to produce paleo-ice sheet reconstructions with minimal assumptions. Geosci. Model Dev 9, 1673–1682. https://doi.org/10.5194/gmd-9-1673-2016

Gregoire, L.J., Otto-Bliesner, B., et al., 2016. Abrupt Bølling warming and ice saddle collapse contributions to the Meltwater Pulse 1a rapid sea level rise. Geophys. Res. Lett. 43, 9130–9137. https://doi.org/10.1002/2016GL070356

Gregoire, L.J., Payne, A.J., Valdes, P.J., 2012. Deglacial rapid sea level rises caused by ice-sheet saddle collapses. Nature 487, 219–222. https://doi.org/10.1038/nature11257

Gregoire, L.J., Valdes, P.J., Payne, A.J., 2015. The relative contribution of orbital forcing and greenhouse gases to the North American deglaciation. Geophys. Res. Lett. 42, 9970–9979. https://doi.org/10.1002/2015GL066005

Gudmundsson, G.H., 2013. Ice-shelf buttressing and the stability of marine ice sheets. Cryosph. 7, 647–655. https://doi.org/10.5194/tc-7-647-2013

Hindmarsh, R.C.A., 2006. The role of membrane-like stresses in determining the stability and sensitivity of the Antarctic ice sheets: back pressure and grounding line motion. Philos. Trans. A. Math. Phys. Eng. Sci. 364, 1733–67. https://doi.org/10.1098/rsta.2006.1797

Hubbard, A., Bradwell, T., et al., 2009. Dynamic cycles, ice streams and their impact on the extent, chronology and deglaciation of the British–Irish ice sheet. Quat. Sci. Rev. 28, 758–776. https://doi.org/10.1016/j.quascirev.2008.12.026

Hughes, A.L.C., Gyllencreutz, R., et al., 2016. The last Eurasian ice sheets - a chronological database and time-slice reconstruction, DATED-1. Boreas 45. https://doi.org/10.1111/bor.12142

Ivanovic, R.F., Gregoire, L.J., et al., 2016. Transient climate simulations of the deglaciation 21–9 thousand years before present (version 1) – PMIP4 Core experiment design and boundary conditions. Geosci. Model Dev. 9, 2563–2587.

https://doi.org/10.5194/gmd-9-2563-2016

Iyengar, G.R., Ramesh, K.J., et al., 2001. Rapid Bottom Melting Widespread near Antarctic Ice Sheet Grounding Lines. Curr. Sci. Nat. Nat. Paleoceanogr. Geol. Geol. Nat. Quat. Res. Nat. Nat. J. Oman Stud. Spec. Rep. J. Maizels, J. Oman Stud. Spec. Rep. Earth Planet. Sci. Lett. M. Ross. Nat. Quat. Sci. Rev. USGS Prof. Pap. Sci. Mar. Geol 80, 61–401.

5 Jamieson, S.S.R., Vieli, A., et al., 2012. Ice-stream stability on a reverse bed slope. Nat. Geosci. 5, 799–802. https://doi.org/10.1038/ngeo1600

Jenkins, A., Dutrieux, P., et al., 2010. Observations beneath Pine Island Glacier in West Antarctica and implications for its retreat. Nat. Geosci. 3, 468–472. https://doi.org/10.1038/ngeo890

Joughin, I., Smith, B.E., & Medley, B., 2014. Marine Ice Sheet Collapse Potentially Under Way for the Thwautes Glacier.
10   Science (80-.). 344, 735–738. https://doi.org/10.1126/science.1249055

Joughin, I., Howat, I.M., et al., 2008. Continued evolution of Jakobshavn Isbrae following its rapid speedup. J. Geophys. Res. 113, F04006. https://doi.org/10.1029/2008JF001023

Matsuoka, K., Hindmarsh, R.C.A., et al., 2015. Antarctic ice rises and rumples: Their properties and significance for ice-sheet dynamics and evolution. Earth Sci. Rev. 150, 724–745. https://doi.org/10.1016/j.earscirev.2015.09.004

15 Morris, P.J., Swindles, G.T., et al., 2018. Global peatland initiation driven by regionally asynchronous warming. Proc. Natl. Acad. Sci. 201717838. https://doi.org/10.1073/pnas.1717838115

Nias, I.J., Cornford, S.L., Payne, A.J., 2016. Contrasting the Modelled sensitivity of the Amundsen Sea Embayment ice streams. J. Glaciol. 62, 552–562. https://doi.org/10.1017/jog.2016.40

Oster, J.L., Ibarra, D.E., et al., 2015. Steering of westerly storms over western North America at the Last Glacial Maximum.
20   Nat. Geosci. 8, 201–205. https://doi.org/10.1038/ngeo2365

Patton, H., Hubbard, A., et al., 2017. Deglaciation of the Eurasian ice sheet complex. Quat. Sci. Rev. 169, 148–172. https://doi.org/10.1016/j.quascirev.2017.05.019

Patton, H., Hubbard, A., et al., 2016. The build-up, configuration, and dynamical sensitivity of the Eurasian ice-sheet complex to Late Weichselian climatic and oceanic forcing. Quat. Sci. Rev. 153, 97–121.
25   https://doi.org/10.1016/j.quascirev.2016.10.009

Pattyn, F., Schoof, C., et al., 2012. Results of the Marine Ice Sheet Model Intercomparison Project, MISMIP. Cryosph. 6, 573–588. https://doi.org/10.5194/tc-6-573-2012

Pope, V.D., Gallani, M.L., et al., 2000. The impact of new physical parametrizations in the Hadley Centre climate model: HadAM3. Clim. Dyn. 16, 123–146. https://doi.org/10.1007/s003820050009

30 Pritchard, H.D., Ligtenberg, S.R.M., et al., 2012. Antarctic ice-sheet loss driven by basal melting of ice shelves. Nature 484, 502–505. https://doi.org/10.1038/nature10968

Ritz, C., Edwards, T.L., et al., 2015. Potential sea-level rise from Antarctic ice-sheet instability constrained by observations. Nature 528, 115–118. https://doi.org/10.1038/nature16147

Ross, N., Bingham, R.G., et al., 2012. Steep reverse bed slope at the grounding line of the Weddell Sea sector in West

Antarctica. Nat. Geosci. 5, 393–396. https://doi.org/10.1038/ngeo1468

Scambos, T.A., Bohlander, J.A., et al., 2004. Glacier acceleration and thinning after ice shelf collapse in the Larsen B embayment, Antarctica. Geophys. Res. Lett. 31, L18402. https://doi.org/10.1029/2004GL020670

Schoof, C., 2007. Ice sheet grounding line dynamics: Steady states, stability, and hysteresis. J. Geophys. Res. 112, F03S28. https://doi.org/10.1029/2006JF000664

Schoof, C., Hindmarsh, R.C.A., 2010. Thin-film flows with wall slip: An asymptotic analysis of higher order glacier flow models. Q. J. Mech. Appl. Math. 63, 73–114. https://doi.org/10.1093/qjmam/hbp025

Seguinot, J., 2013. Spatial and seasonal effects of temperature variability in a positive degree-day glacier surface mass-balance model. J. Glaciol. 59, 1202–1204. https://doi.org/10.3189/2013JoG13J081

Siegert, M.J., Dowdeswell, J.A., 2004. Numerical reconstructions of the Eurasian Ice Sheet and climate during the Late Weichselian. Quat. Sci. Rev. 23, 1273–1283. https://doi.org/10.1016/J.QUASCIREV.2003.12.010

Singarayer, J.S., Valdes, P.J., et al., 2011. Late Holocene methane rise caused by orbitally controlled increase in tropical sources. Nature 470, 82–86. https://doi.org/10.1038/nature09739

Singarayer, J.S., Valdes, P.J., 2010. High-latitude climate sensitivity to ice-sheet forcing over the last 120 kyr. https://doi.org/10.1016/j.quascirev.2009.10.011

Stoker, M.S., Bradwell, T., 2005. The Minch palaeo-ice stream, NW sector of the British–Irish Ice Sheet. J. Geol. Soc. London. 162, 425–428. https://doi.org/10.1144/0016-764904-151

Swindles, G.T., Morris, P.J., et al., 2017. Ecosystem state shifts during long-term development of an Amazonian peatland. Glob. Chang. Biol. https://doi.org/10.1111/gcb.13950

Valdes, P.J., Armstrong, E., et al., 2017. The BRIDGE HadCM3 family of climate models: HadCM3@Bristol v1.0. Geosci. Model Dev. 10, 3715–3743. https://doi.org/10.5194/gmd-10-3715-2017

van der Veen, C.J., 2013. Fundamentals of glacier dynamics, CRC Press. CRC Press. https://doi.org/10.3189/2014JoG13J214
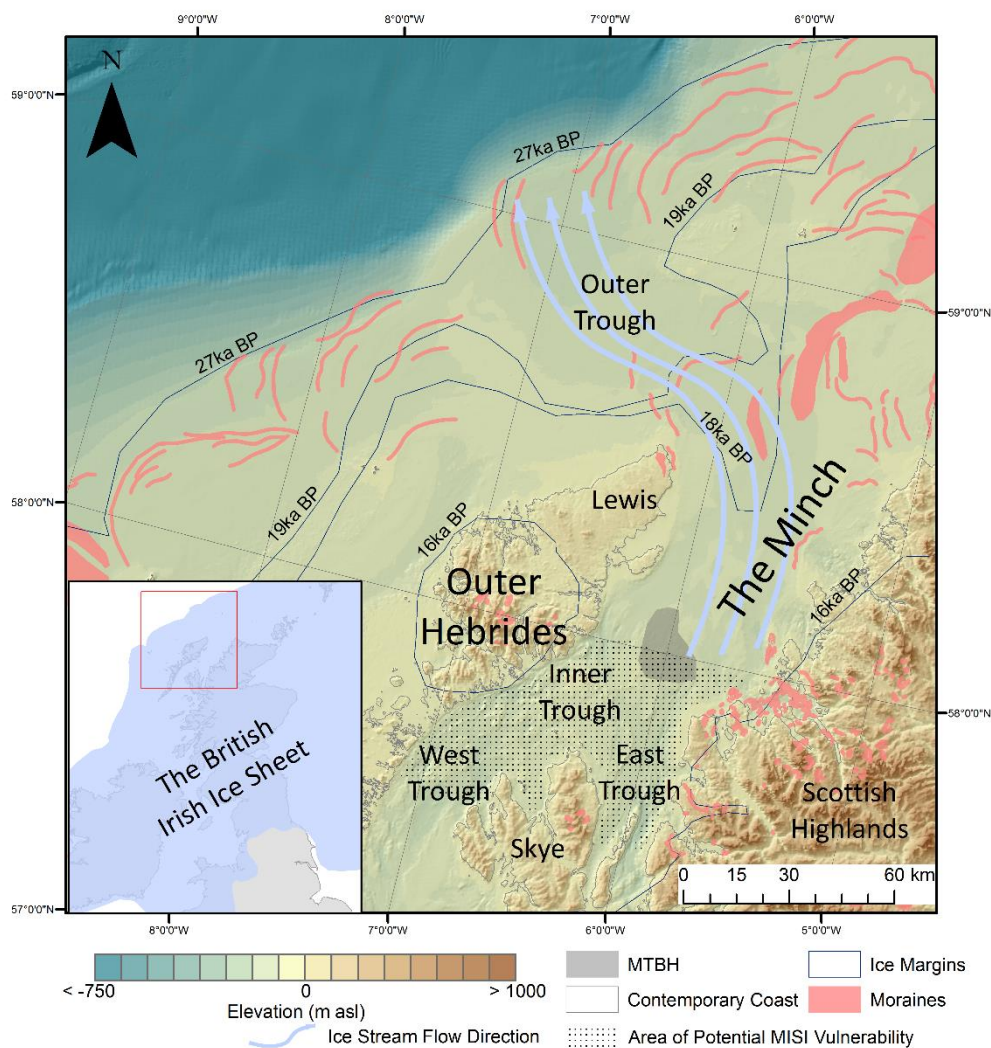
Figure 1: Location and geographical setting of the Minch Ice Stream. The inset shows the maximum extent of the British-Irish Ice Sheet from Clark et al. (2012). The red box indicates the Minch ice stream region shown in the larger map. Ice margins and dates are from Clark et al. (2012). Moraines are from the BRITICE glacial landform map, version 2 (Clark et al., 2018). Area of potential MISI vulnerability is inferred from the presence of marine retrograde slopes. Key locations mentioned in the text are labelled.
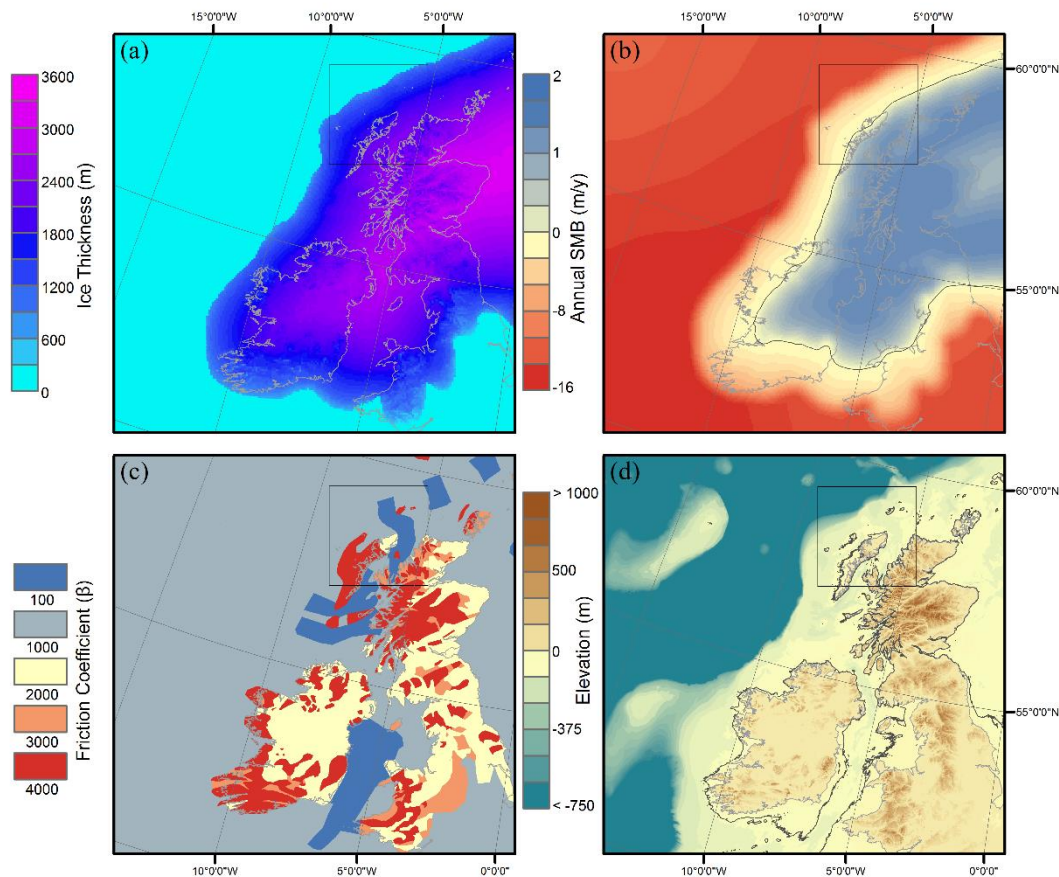
Figure 2: Initial conditions and boundary conditions for the equilibrium spin-up lLGM ice sheet simulation, showing the full domain of the simulations. (a) Initial ice thickness (m), (b) Annual Surface Mass Balance (m/y), with black contour line representing the Equilibrium Line (SMB = 0 m/y). (c) Bed Friction Coefficient (β), d) Isostatically adjusted topography (m) corresponding to 30 ka BP. The maps show the full ice sheet domain and the black boxes indicate the area of model grid refinement referred to as the Minch sector.
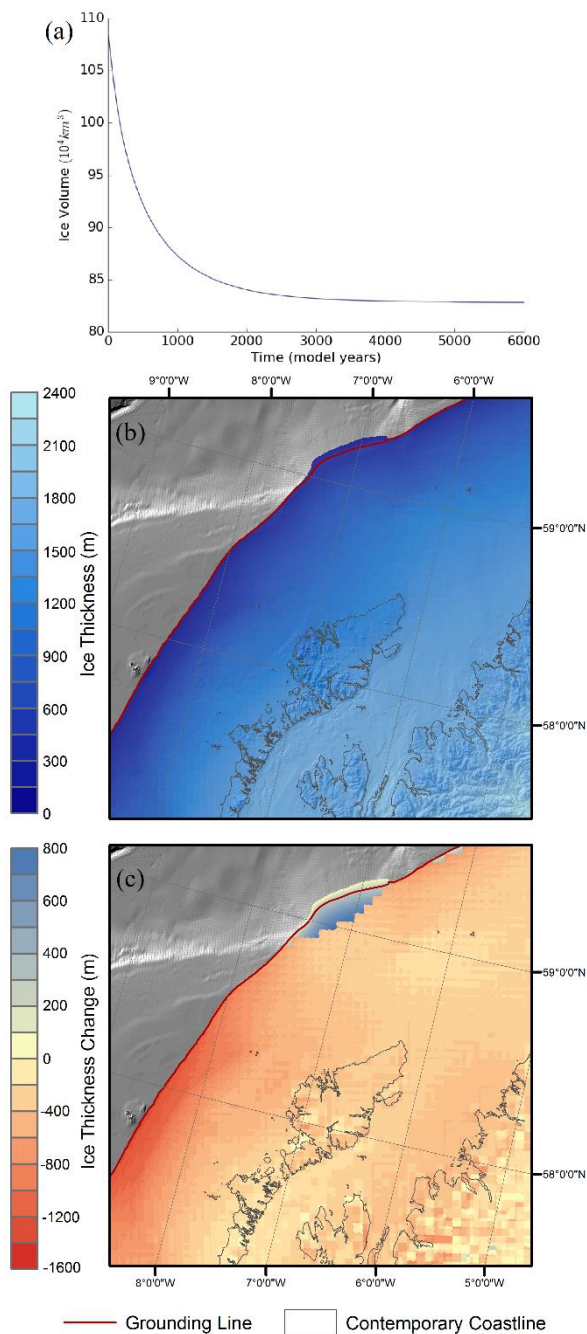
Figure 3: a) Evolution of the ice sheet volume over the Minch sector during spin-up. b) Simulated ice sheet thickness after 6,000 model years of spin-up, c) Ice thickness change between the start and end (year 6000) of the spin-up simulation (i.e. difference between Figure 2a and Figure 3b.)
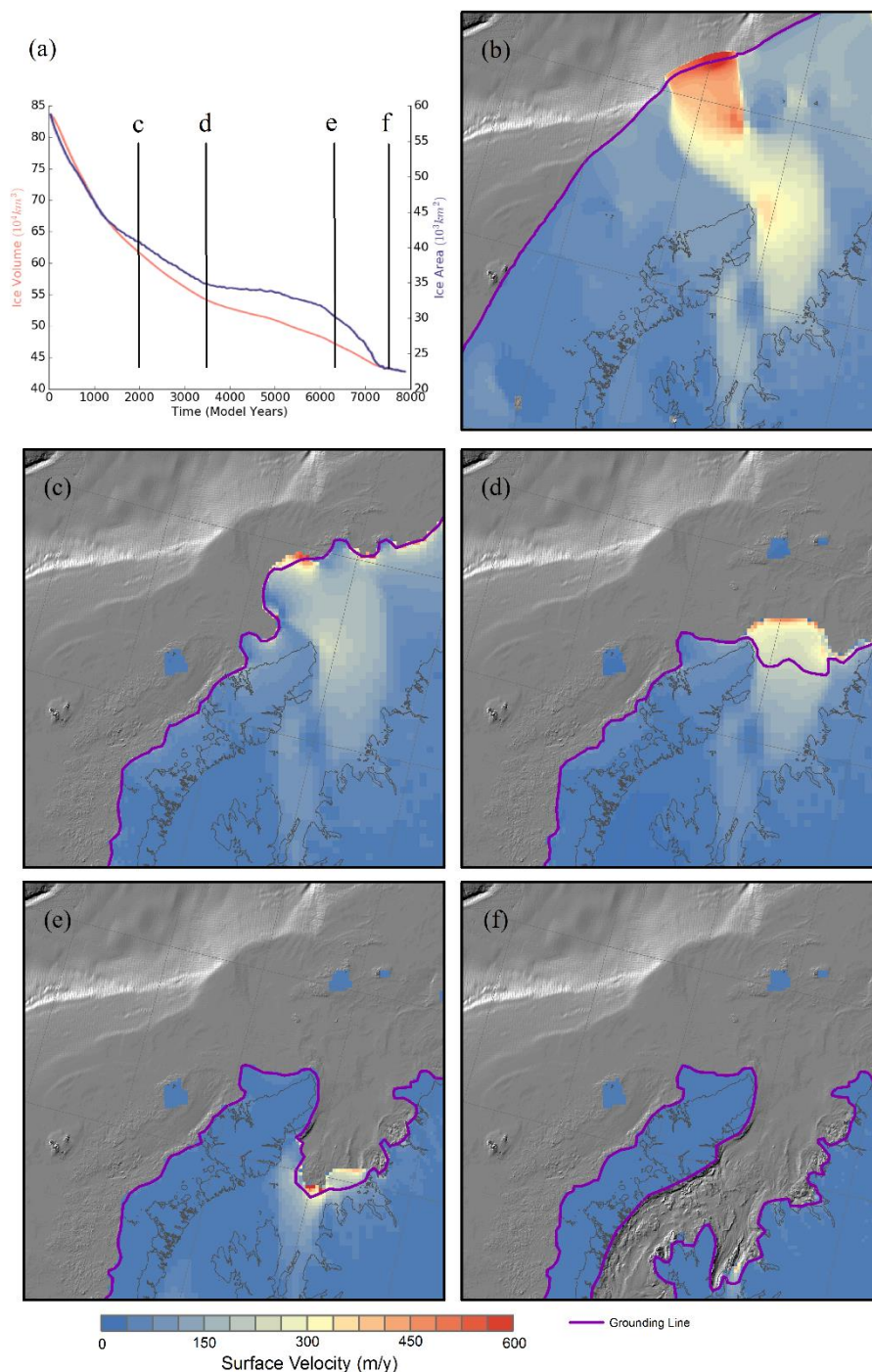
Figure 4: Evolution of the ice sheet in the Minch sector in the _RETREAT_ simulation. a) Timeseries of ice volume and area over the Minch sector. Ice surface velocity (b, c, d, e, and f) at 0, 2000, 3500, 6300, and 7500 model years respectively with grounding line shown in purple.
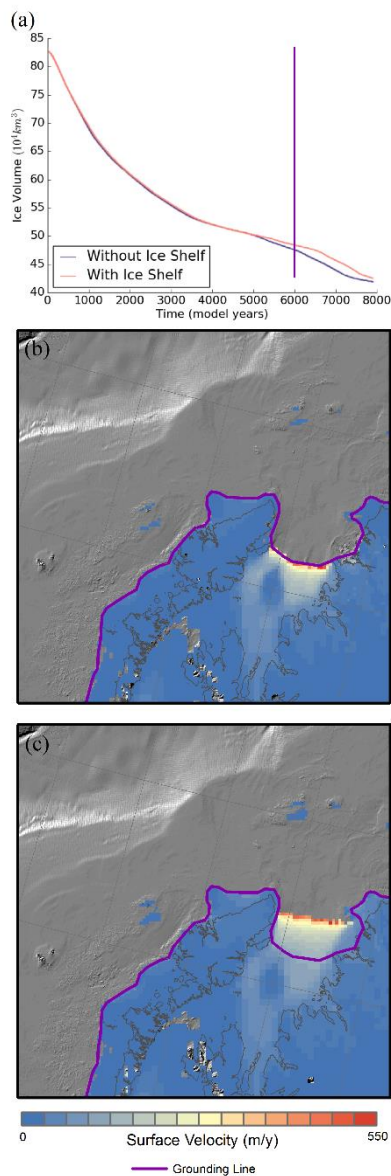
Figure 5: Effect of ice shelves. (a) Evolution of ice sheet volume over the Minch sector in simulation _RETREAT_ with ice shelves (red line) and _RETREAT_NOSHELF_ in which ice shelves are forcibly removed (blue line). (b,c) Surface velocity and grounding line location (purple line) in RETREAT_NOSHELF (b) and _RETREAT_ (c).
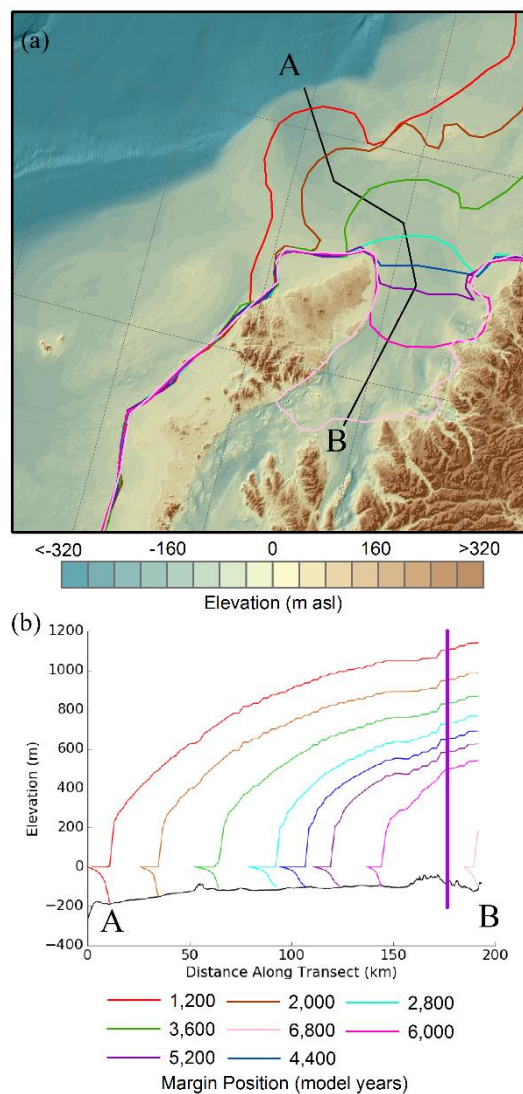
Figure 6: a) The grounding line position of the ice sheet at 800 year intervals during the *RETREAT* simulation. b) Transect through the ice stream showing the ice sheet elevation at the same intervals. The purple line marks the grounding line position in the stable "collapsed" ice sheet state from the *READVANCE* simulations (Figure 7d).
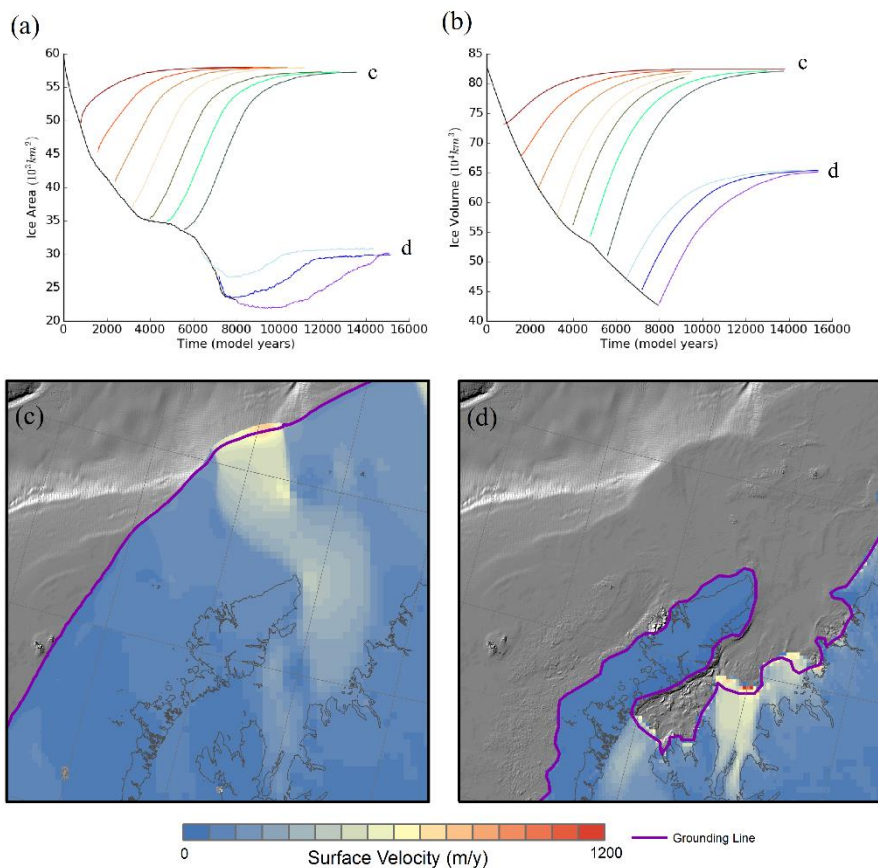
Figure 7: Results of the ensemble of *READVANCE* simulations testing instability in the Minch Ice Stream. (a,b) Evolution of the ice sheet area (a) and volume (b) over the Minch sector in the *RETREAT* (black) and *READVANCE* simulations (coloured lines). Labels c and d indicate the "maximum" (c) and "collapsed" (d) stable states with corresponding panels showing the respective surface ice sheet velocity (m/y) and grounding line locations (purple line).
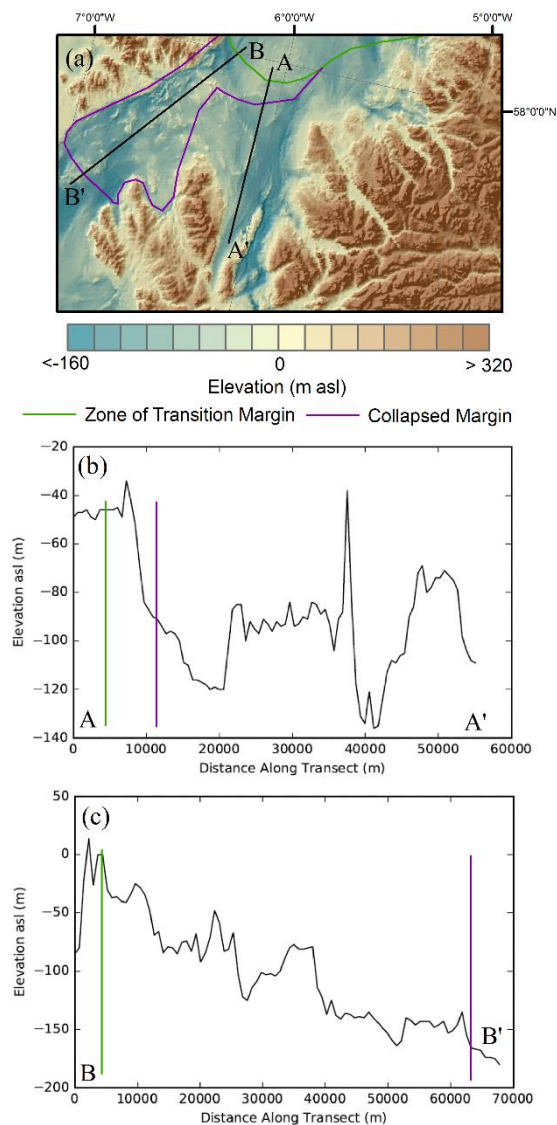
Figure 8: The difference in the effects of MISI between the East Trough and the West Trough. a) 6,400 model year *RETREAT* margin (green) and the stable "collapsed" extent margin (purple). b) A-A' transect of bathymetry and collapse extent in the East Trough. c) B-B' transect of bathymetry and collapse extent in the West Trough.